Biochemical and Biophysical Research Communications 395 (2010) 509–514

Contents lists available at ScienceDirect

Biochemical and Biophysical Research Communications

journal homepage: www.elsevier.com/locate/ybbrc

Molting-specific downregulation of *C. elegans* body-wall muscle attachment sites: The role of RNF-5 E3 ligase

Ronen Zaidel-Bar [a], Shahar Miller [b], Rachel Kaminsky [b], Limor Broday [b,*]

[a] Department of Cell and Developmental Biology, Sackler School of Medicine, Tel-Aviv University, Tel-Aviv 69978, Israel
[b] Zoology Department, University of Wisconsin – Madison, Madison, WI 53706, USA

ARTICLE INFO

Article history:
Received 26 March 2010
Available online 10 April 2010

Keywords:
Molting
Lethargus
Muscle dense bodies
Caenorhabditis elegans

ABSTRACT

Repeated molting of the cuticula is an integral part of arthropod and nematode development. Shedding of the old cuticle takes place on the surface of hypodermal cells, which are also responsible for secretion and synthesis of a new cuticle. Here, we use the model nematode *Caenorhabditis elegans* to show that muscle cells, laying beneath and mechanically linked to the hypodermis, play an important role during molting. We followed the molecular composition and distribution of integrin mediated adhesion structures called dense bodies (DB), which indirectly connect muscles to the hypodermis. We found the concentration of two DB proteins (PAT-3/β-integrin and UNC-95) to decrease during the quiescent phase of molting, concomitant with an apparent increase in lateral movement of the DB. We show that levels of the E3-ligase RNF-5 increase specifically during molting, and that RNF-5 acts to ubiquitinate the DB protein UNC-95. Persistent high levels of RNF-5 driven by a heatshock or *unc-95* promoter lead to failure of ecdysis, and in non-molting worms to a progressive detachment of the cuticle from the hypodermis. These observations indicate that increased DB dynamics characterizes the lethargus phase of molting in parallel to decreased levels of DB components and that temporal expression of RNF-5 contributes to an efficient molting process.

1. Introduction

Molting animals (ecdysozoans), such as nematodes and arthropods, form the largest group in the animal kingdom [1], including many human and agricultural parasites and pathogens [2]. In developing defenses against such parasites molting is an attractive target. While not parasitic itself, the nematode *Caenorhabditis elegans* serves as an excellent genetic model for the study of molting.

Between hatching and adulthood, the nematode *C. elegans* will grow fourfold in length and undergo four molts [3]. During each molt the old cuticle (exoskeleton) must separate from the epidermis before new cuticle material can be deposited (apolysis) [4]. At this time the worm enters a sleep-like quiescence termed lethargus [5]. Epidermal growth factor signaling in neurons is responsible for the cessation of pharyngeal pumping and locomotion that occurs during the lethargus period [6].

Cholesterol and steroid hormones signal to initiate molting [7,8], likely through nuclear hormone receptors [9,10], and low density lipoprotein receptors [11]. Metalloproteases and other proteases have essential roles in removal of the old cuticle [12,13].

Hypodermal cells are responsible for production and secretion of a multitude of extracellular matrix (ECM) proteins, primarily collagens, to form the new cuticle [4]. Once the new cuticle is in place, about 2 h later, intense muscle-driven twisting and turning facilitate the worm's escape from inside its old cuticle (ecdysis) [4].

A recent genome wide RNAi screen by Frand et al. found 159 genes in *C. elegans* whose products were essential for completion of molting. Not surprisingly, among these genes were transcription factors, proteases, signaling proteins, and ECM components of the cuticle [14]. Less expected was the discovered involvement in molting of muscle tropomyosin and *unc-52*/Perlecan, which is the ECM substrate of muscle dense bodies (DB).

DB are integrin based cell-ECM adhesion structures homologous to vertebrate focal adhesions [15]. UNC-52/Perlecan, a heparan sulfate proteoglycan, is required for the clustering and activation of PAT-2/α-integrin and PAT-3/β-integrin [16], which is followed by the recruitment of DB components such as PAT-4/ILK, talin, UNC-97/PINCH, UNC-95, DEB-1/vinculin, and PAT-6/actopaxin [17]. Within the muscle cells DB connect integrins with the actin filaments (Z-bands) of the sarcomere. The actin filaments, coupled with alternating myosin filaments (M-lines), provide the contractile forces of the muscle [17].

Caenorhabditis elegans body-wall muscle cells lay beneath the hypodermis, separated by approximately 40–80 nm of ECM

* Corresponding author. Fax: +972 3 640 7432.
E-mail address: broday@post.tau.ac.il (L. Broday).

0006-291X/$ - see front matter © 2010 Elsevier Inc. All rights reserved.
doi:10.1016/j.bbrc.2010.04.049

(http://www.wormatlas.org/). DB integrins attach muscle cells to the inside surface of this ECM, while hypodermal cells are tethered along their basal membrane to the outer surface of the same ECM via hemidesmosome-like structures called fibrous organelles (FO) [15,18]. LET-805/myotactin is the transmembrane receptor on the basal side of the FO [19]. The pillar-like structure of FO is composed of intermediate filaments and VAB-10/plectin [20,21] and is connected on the apical side of the hypodermal cell with the cuticle via MUA-3 and MUP-4 transmembrane proteins [22,23]. Interestingly, LET-805/myotactin and MUP-4 are also necessary for proper molting [14].

Thus, albeit not directly, the muscle is mechanically linked to the hypodermis and cuticle. This physical coupling is necessary for locomotion, and several lines of evidence suggest that it may also play a role in mechanically induced signalling in the hypodermis. Without muscle activity embryonic development is arrested at the twofold stage [24], even though it is thought that the elongation process is driven by hypodermal cells [25]. Recently it was shown that gene expression in the hypodermis is affected by mutations in the DB protein UNC-95 [26]. Strikingly, the hypodermal genes whose expression was most dramatically affected in the *unc-95* mutant all have a role in cuticle synthesis and molting [26].

Given the intimate relationship between muscles and the hypodermis this study examined the regulation of muscle DB during molting and asked whether it has an impact on the process of molting.

2. Materials and methods

2.1. Strains

Caenorhabditis elegans strains were grown at 20 °C according to standard protocols [27]. The wild-type strain used is Bristol N2. The following transgenes were used: *rhIs2*[PAT-3::HA::GFP] [28], *ryIs22* [UNC-95::GFP;*rol-6*] [29], *tvIs24*[*hsp-16p*::RNF-5;*rol-6*] (this study), *tvEx49*[*unc-95p*::RNF-5;*myo-2p*::GFP] (this study), *tvEx48* [*hsp-16p*::RNF-5;*myo-2p*::GFP];*ryIs22* (this study).

2.2. In vitro ubiquitination

For in vitro ubiquitination of UNC-95::GFP, worms pellets from the *ryIs22* [UNC-95::GFP;*rol-6*] strain were incubated with equal volume of lysis buffer (100 mM NaCl, 50 mM NaF, 50 mM Tris pH 7.5, 1 mM EGTA, 5% glycerol, 1% Nonidet P40, 1 mM DTT, 10 μg/ml leupeptin, 10 μg/ml aprotinin, 10 μg/ml pepstatin A) on ice followed by sonication (5 s, 5 times). Samples were centrifuged (15 min, 14000 rpm) and supernatants were pre-cleared by incubation with protein G beads (Roche) (30 min at 4 °C), followed by incubation with anti-GFP antibody (Roche) (1 h at 4 °C). Immunoprecipitation was performed by incubation (2 h at 4 °C) with protein G beads (Roche). Beads were washed with 30 mM Tris pH 7.6, 50 mM NaCl, 5 mM MgCl2, 1 mM DTT and a sample was used for the IP lane (lane 1, 25% of the immunoprecipitate used in each ubiquitination reaction). Ubiquitination reactions were performed in 1× ubiquitination buffer (30 mM Tris pH 7.6, 50 mM NaCl, 5 mM MgCl2, 1 mM DTT, 2 mM ATP, 1 mM HA-ubiquitin) including 200 ng E1 (Biomol), 200 ng E2 (bacterially expressed and purified His-UBCH5c) and 200 ng GST-RNF-5 for 15 min at 37 °C. Reactions were terminated with 8 M urea, 0.1 M Na_2HPO_4/NaH_2PO_4 (pH 6.3), 0.1% Nonidet P40 and washed four times with the lysis buffer. Proteins were solubilized in 3× Laemmli buffer and separated on SDS–PAGE followed by immunoblot analysis with the indicated antibodies.

2.3. Antibodies

Antibodies used for Western analysis are anti-RNF-5 (1:4000), anti-GFP (Roche) (1:7000) anti HA (Roche) (1:10,000), anti-actin (Santa Cruz) (1:3000).

2.4. Microscopy and quantification

Worms were mounted on 4% agarose pads and anesthetized with 0.1% tricaine and 0.01% tetramisole. Confocal analysis of UNC-95::GFP and PAT-3::GFP expression was performed using a Zeiss LSM 5 EXCITER confocal scanning microscope using a 63× NA1.4 objective lens. In Fig. 1A and B a single focal plane at the base of the DB was recorded in each worm (pixel time 6.4 μs, image size ~32 × 4.6 μm). Filtration of the images was done using ImageJ (rolling ball background subtraction, radius = 10 pixels). Line profiles were calculated using ImageJ. Analysis of line profiles was done for 10 worms of each condition (at least 10 DB/worm). Peak intensity values of each DB in all line profiles were found and the mean and standard deviation values were calculated.

For the analysis shown in Fig. S1 stack of 10–13 focal planes (image size ~47 × 23 × 3 μm, pixel time 6.4 μs) was captured starting at the muscle cell membrane through the depth of the body-wall muscle cells. Images showing a single focal plane at the base of the muscle attachments and a single focal plane of muscle nuclei are shown for each developmental stage. At least 10 worms from each stage were imaged and representative images are shown.

Time lapse imaging was carried out using a Zeiss Axiovert 200 equipped with an AxioCam MRm camera. Analysis of DB movement was made using image analysis tools in MATLAB.

The acquired series of images were transformed into series of black and white images, with histogram equalization and conversion to binary images using the default MATLAB Otsu's method. In each frame, DBs were identified using binary labeling. Size and shape constraints were applied to filter out noise and artifacts. The trajectory of each DB was tracked using frame-to-frame matching subjected to DB movement limitations and restrictions. Specifically, if a DB location could not be found in any frame the DB was discarded from the analysis. Given the DB locations in all the frames, its trajectory was identified. The average between-frame movement of all the DBs in any worm was calculated and taken to represent the whole-worm movement. This frame-by-frame average motion was subtracted from each DB trajectory, to filter out the whole-worm movement. The residual DB movement is assumed to represent the specific DB movements. At least five worms (10 DB/worm) were analyzed in each condition.

For the analysis shown in Fig. 4, at least 20 worms were analyzed in each condition and representative images are shown. In mid and bottom panels of (E) and in (F), high PMT gain conditions were used due to weak and diffuse GFP signal in the DB.

3. Results and discussion

3.1. UNC-95 and PAT-3/beta-integrin levels in dense bodies decrease during molting

To test whether DB undergo any change during molting we examined by fluorescence confocal microscopy the localization in DB of two GFP fusion proteins: PAT-3/β-integrin::GFP and UNC-95::GFP. We chose worms during the L2-L3 molt, identified by their lethargus behavior, and compared them with worms in the L3 stage. In non-molting animals we observed for both markers the known pattern of DB, which is characterized by equally spaced spots about 0.6 μm in diameter laying along imaginary straight

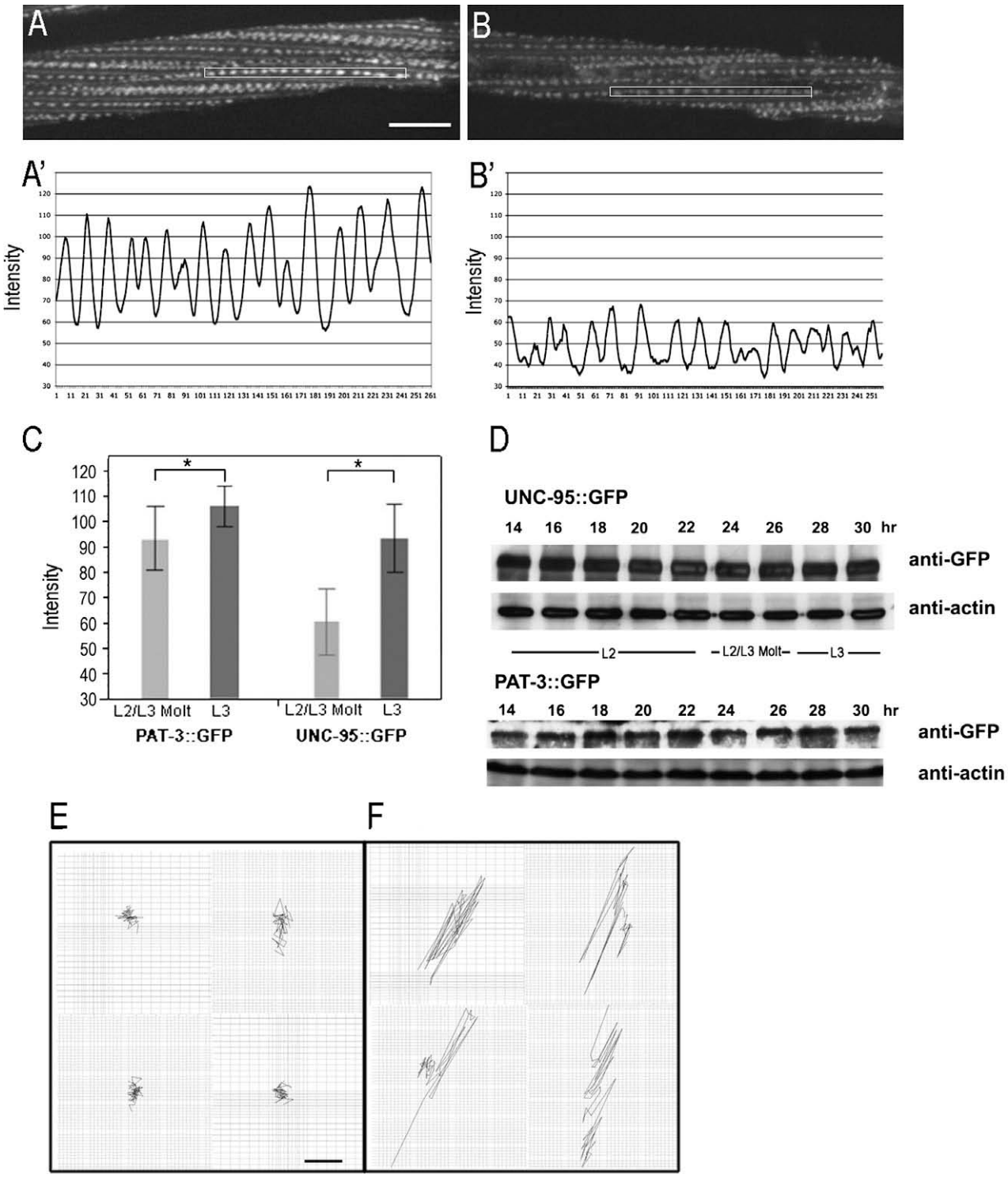

Fig. 1. Adaptor protein levels in DB decrease during molting, as DB become less organized and more dynamic. (A) UNC-95::GFP in L3 worms. The intensity profile along the boxed DB is shown in A′. (B) UNC-95::GFP in a lethargus worms during L2/L3 molt. The intensity profile in B′ shows that during molting the pattern of the DB is disrupted by lower peaks as well as unequal spacing between peaks. Bar, 5 μm. (C) Quantification of the average fluorescent intensity of PAT-3 and UNC-95 in individual DB in L3 or in L2/L3 molt. Bars denote standard deviation. Asterisks mark statistical significance (Student's *t*-test). (D) Western blot analysis of total worm proteins of the UNC-95::GFP and PAT-3::GFP strains at 14–30 h post-L1 arrest. Worms were grown at 20 °C. The L2/L3 occurs between 24 and 26 h after release from L1 arrest. (E) Trajectory plots of four individual DB followed for 60 s at 200 ms intervals in anesthetized L3 worms. (F) Same as E, but in L2/L3 molt. Bar, 0.2 μm.

lines (Fig. 1A). Fluorescence intensity profiles drawn along such lines show very low diffusive levels and narrow peaks across each DB (Fig. 1A′). UNC-95-GFP showed a 36% decrease in average intensity at the DB during molting (Fig. 1B). We observed a more modest yet statistically significant 12% decrease in the average intensity of PAT-3/β-integrin-GFP (Fig. 1C). This probably means the downregulation of DB is manifested by a reduction in adaptor proteins and has a smaller effect on the number of integrin receptors in DB.

Western blot analysis using anti-GFP antibodies indicated there were no changes in total protein levels of UNC-95:GFP or

PAT-3:GFP during molting, suggesting the observed reduction in intensity is due to changes in localization (Fig. 1D). Accordingly, additional confocal analysis of UNC-95::GFP expression in body-wall muscles at molt (L2/L3) and intermolt larvae (L2 and L3) showed that decrease in DB intensity during the lethargus phase is accompanied by a diffuse signal at muscle attachment sites, but with no major changes in cytosolic and nuclear fluorescence levels (Fig. S1).

In addition to the changes in intensity we noticed the pattern of DB was less organized during molting, i.e., the distance between adjacent DB was not as uniform as in the non-molting controls (Figs. 1B and S1, left panels). This observation could be explained if the DB in molting animals are able to move more freely within the lattice of actin and myosin.

3.2. During molting dense bodies become less organized and display larger displacements

To directly address the issue of DB movement within the sarcomere we imaged PAT-3/β-integrin-GFP in anesthetized living worms during and after the L2/L3 molt. Even under anesthetic conditions some small muscle contractions still occur. Therefore, we developed a computer program that allows us to follow the movement of cohorts of DB and separate between movements of the whole cell or sarcomere contraction and the smaller fluctuations in position of individual DB. Using this tool we observed DB to move larger distances during molting. In 1 min movies at a time resolution of 200 ms DB in non-molting animals made small movements, but remained confined to a radius of 0.2 μm around the center of DB (Fig. 1E). In contrast, during molting DB were observed to fluctuate in position more than 1 μm and they did not appear to return necessarily to the same point (Fig. 1F).

The observed increase in DB displacement could be explained by two, not mutually exclusive, mechanisms: increased flexibility of the ECM due to the disengagement of the cuticle and increased freedom within the sarcomere due to fewer connections with actin filaments. The reason for weaker connections with actin may be the reduced levels of adaptor proteins, such as UNC-95, in the DB, raising the question of how their levels are regulated. One attractive possibility is that DB levels of UNC-95 and possibly other adaptors are regulated by the E3-ligase RNF-5.

3.3. UNC-95 is a target for ubiquitination by RNF-5 E3 ligase

The LIM-domain protein UNC-95 was originally isolated as an interactor with worm RNF5 in a yeast two hybrid screen, and subsequently it was shown that UNC-95 localization was regulated by RNF-5 [29]. Over-expression of RNF-5 led to a marked reduction in UNC-95 levels, and conversely, knockdown of RNF-5 by RNAi led to an increase in UNC-95 levels in muscle cells [29]. Recent works in mammalian cells and in *Xenopus* have shown that ubiquitination of the LIM-domain protein paxillin by RNF-5 homologs RNF5 and RNF185, respectively, lead to its mislocalization from focal adhesions [30,31]. To specifically test whether UNC-95 is a target for ubiquitination by worm RNF-5 we performed in vitro ubiquitination assays. To this end, UNC-95::GFP was immunoprecipitated using anti-GFP antibody from UNC-95::GFP transgenic worms, and the immune-purified UNC-95::GFP was then subjected to in vitro ubiquitination assay, using bacterially expressed GST-RNF-5 in the presence of HA-tagged ubiquitin. This reaction resulted in the formation of high-molecular-weight conjugates that were recognized by antibodies to HA. This data provides direct evidence for the ubiquitination of UNC-95::GFP by RNF-5 (Fig. 2).

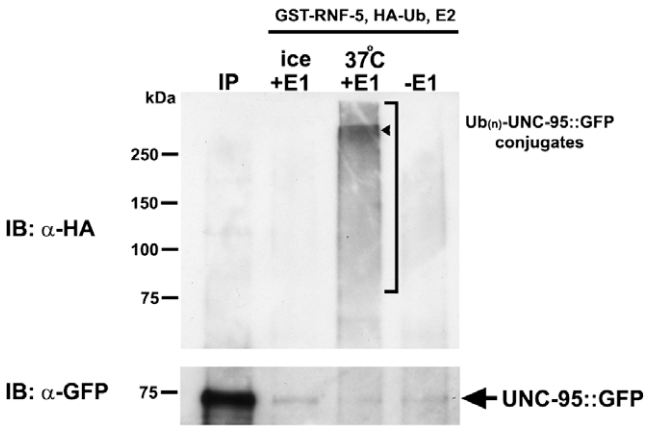

Fig. 2. UNC-95 is a substrate for RNF-5 E3 ligase activity. Western blots of in vitro ubiquitination of UNC-95::GFP immunoprecipitated from UNC-95::GFP worms. Equal aliquots of immunopurified UNC-95::GFP were used in each reaction in the presence of bacterially expressed and purified GST-RNF-5, E2, HA-ubiquitin and ATP, with or without E1 as indicated. Reactions were incubated at 37 °C or on ice for 15 min and terminated with 8 M urea buffer. The ubiquitinated forms of UNC-95::GFP are indicated by parentheses. Arrowhead indicates the 5% stacking gel-8% running gel boundary. Arrow indicates UNC-95::GFP. IP, 25% of the immunoprecipitate used in each ubiquitination reaction (unwashed).

3.4. RNF-5 protein levels increase during molting and must decrease for proper ecdysis

Next, we examined the temporal expression pattern of RNF-5 during larval development by Western analysis using a specific antibody against RNF-5. Quite strikingly, RNF-5 protein levels are low before and after molting and very high during the molting period (Fig. 3). In light of our observations in DB of decreased intensity and increased dynamics during molting and our data showing UNC-95 to be a direct target of RNF-5, it appears likely that RNF-5 expression during molting serves as a "clutch" to decouple muscle contractions from the cuticle during lethargus, when the worm must lay motionless.

Is the molting-specific expression of RNF-5 essential for successful molting? Knockdown of *rnf-5* by RNAi as well as the deletion allele *rnf-5(tm794)* did not result in any molting defects (data not shown). This is likely due to compensation by the activity of other E3 ligases in the muscle at this time. However, we found that a precise timing of RNF-5 activity is necessary for the completion of the molting process. Specifically, over-expression of RNF-5 using the *hsp-16* heat shock promoter lead to molting defects (the Mlt phenotype) in which the old cuticle failed to shed at ecdysis. Old cuticle was observed extending from the anterior end of the worm, and in many cases larvae failed to shed cuticle lining the buccal cavity (Fig. 4A). Heat shock at the beginning of the L1 or L2 phase caused damage to the hypodermal/cuticle attachment (Mua phenotype, muscle attachment abnormal) (Fig. 4B). Increased RNF-5 levels during the period when *rnf-5* is normally expressed

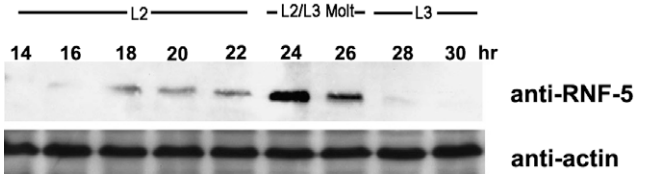

Fig. 3. Endogenous RNF-5 is expressed strictly during molting. Western blot analysis of total worm proteins of the UNC-95::GFP strain at 14–30 h post-L1 arrest. Worms were grown at 20 °C. Molting occurs between 24 and 26 h after release from L1 arrest.

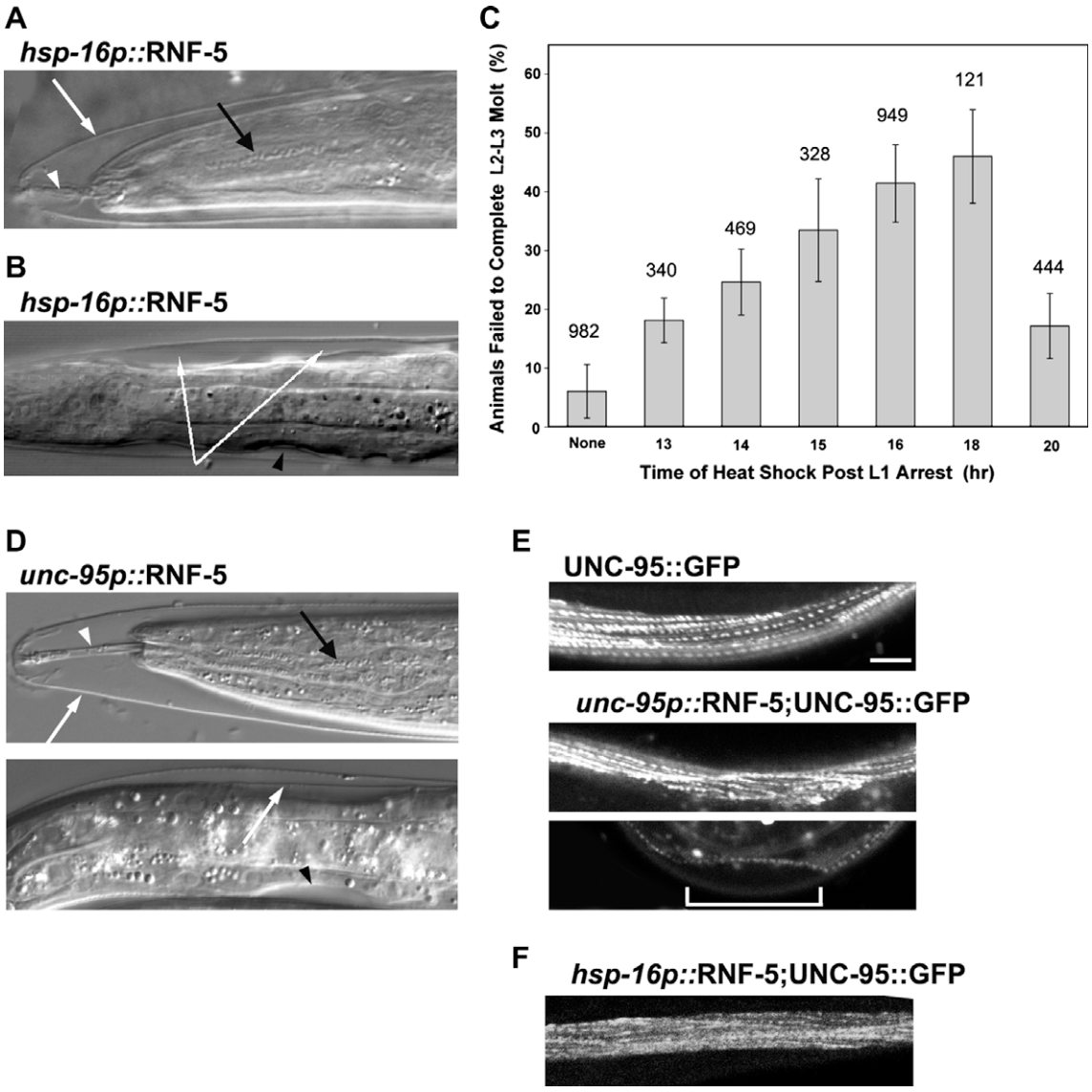

Fig. 4. Over-expression of RNF-5 results in molting defects. (A,B) Induction of RNF-5 during the second larval stage. (A) Mid-L2 and (B) early L2. Larva encased in its old cuticle or double cuticle (white arrow), the expelled pharyngeal cuticle (white arrowhead), accumulation of granules within the pharyngeal gland ducts (black arrow), separation of the cuticle (black arrowhead) (C) The level of Mlt phenotype depends on the timing of RNF-5 induction during the second larval stage. Mean values and standard deviation from three independent experiments are shown. *n*, total number of worms analyzed (indicated above each bar) (D) Expression of RNF-5 in the body-wall muscles through *unc-95* regulatory sequences. (E) Expression pattern of the UNC-95::GFP reporter in control worms (L3 stage, low PMT gain) and in worms expressing RNF-5 under the regulation of *unc-95* regulatory sequences (L3 stage, high PMT gain). Brackets designates the region along the worm where the muscle cells are detached. (F) Expression pattern of the UNC-95::GFP reporter in worms expressing RNF-5 under the regulation of the *hsp-16* promoter (L3 stage, high PMT gain; compare to Fig. S1 middle panel). Bar, 5 μm.

did not have deleterious effect (Fig. 4C, 20 h; assuming 2–4 h till the protein accumulates to high levels following heat shock). However, induction of RNF-5 before this time point led to varying degrees of failure to complete ecdysis. The strongest effect was seen 6 h before the molt, when 45% of heat shocked worms failed to complete ecdysis (Fig. 4C, 18 h). As control, we treated wild-type (N2) with heat shock in the same time points. No effect on molting was observed following heat shock treatments ($n > 200$ for each time point). In RNF-5 overexpressing worms we observed accumulation of granules within the pharyngeal gland ducts (Fig. 4A and D, black arrow). Such granules are usually secreted just prior to molting and are thought to help loosen the old cuticle [3]. It is possible that high levels of RNF-5 inhibit the transport or exocytosis of these granules/vesicles by downregulation of a transport protein. The effect of RNF-5 over-expression is reversible, and a few hours later the animals escape from the old cuticle and continue development.

The finding that RNF-5 levels must be low before molting is consistent with high RNF-5 levels promoting downregulation of DB, as necessary only during lethargus. Increased expression of RNF-5 prior to molting, may be behaving like a heterochronic mutation, resulting in a delayed or precocious molting phenotype, depending on the timing of RNF-5 expression.

3.5. Ectopic RNF-5 expression in muscle cells is sufficient to perturb molting and downregulates dense bodies

To test whether the effects of forced *rnf-5* expression on molting can be attributed to its specific expression in muscle we drove *rnf-5* expression using the *unc-95* promoter. Under these conditions we observed delay in molting and the Mua phenotype, proving that RNF-5's effect is directly in the muscle (Fig. 4D). To further test whether expression of RNF-5 is responsible for the decrease in DB protein levels and increase in DB dynamics, DB were observed

in anesthetized UNC-95::GFP worms. We found disorganization of the lattice reminiscent of DB during lethargus, signs of detachment of the muscle from the body wall and lower fluorescence levels (Fig. 4E). The same effect was observed when RNF-5 was overexpressed using the heat shock promoter during the L3 stage when normally RNF-5 levels are low (Fig. 4F).

4. Conclusions

Together, these results demonstrate that the composition and dynamics of the muscle DB change during the molting period, supporting a regulatory role for the DB in the molting process. Decrease in the levels of PAT-3, UNC-95 and possibly other DB proteins weaken the link between the muscle and hypodermis and indirectly weaken the connection between the hypodermis and cuticle. The E3 ligase activity of RNF-5 toward DB components as UNC-95 is temporally restricted to the lethargus phase of molting.

Acknowledgments

The authors thank Benjamin Geiger for discussions, John Plenefisch for the *rhIs2*[PAT-3::HA::GFP] strain and Ulrike Bening-Abu-Shach for technical assistance. This study was supported by a Research Career Development Award from the Israel Cancer Research Fund (06-203-RCDA) and a Research Grant by The Israel Science Foundation (980/06) to L.B. R.Z.B. was supported by NIH postdoctoral training Grant GM078747 and by a fellowship from the Machiah Foundation.

Appendix A. Supplementary data

Supplementary data associated with this article can be found, in the online version, at doi:10.1016/j.bbrc.2010.04.049.

References

[1] A.M. Aguinaldo, J.M. Turbeville, L.S. Linford, M.C. Rivera, J.R. Garey, R.A. Raff, J.A. Lake, Evidence for a clade of nematodes, arthropods and other moulting animals, Nature 387 (1997) 489–493.
[2] M. Mitreva, D.S. Zarlenga, J.P. McCarter, D.P. Jasmer, Parasitic nematodes – from genomes to control, Vet. Parasitol. 148 (2007) 31–42.
[3] R. Singh, J. Sulston, Some observations on moulting in *Caenorhabditis elegans*, Nematologica 24 (1978) 63–71.
[4] A.P. Page, I.L. Johnstone, The cuticle, WormBook (2007) 1–15.
[5] D.M. Raizen, J.E. Zimmerman, M.H. Maycock, U.D. Ta, Y.J. You, M.V. Sundaram, A.I. Pack, Lethargus is a *Caenorhabditis elegans* sleep-like state, Nature 451 (2008) 569–572.
[6] C. Van Buskirk, P.W. Sternberg, Epidermal growth factor signaling induces behavioral quiescence in *Caenorhabditis elegans*, Nat. Neurosci. 10 (2007) 1300–1307.
[7] L.M. Kuervers, C.L. Jones, N.J. O'Neil, D.L. Baillie, The sterol modifying enzyme LET-767 is essential for growth, reproduction and development in *Caenorhabditis elegans*, Mol. Genet. Genomics 270 (2003) 121–131.
[8] T.V. Kurzchalia, S. Ward, Why do worms need cholesterol? Nat. Cell Biol. 5 (2003) 684–688.
[9] A. Antebi, Nuclear hormone receptors in *C. elegans*, WormBook (2006) 1–13.
[10] M. Kostrouchova, M. Krause, Z. Kostrouch, J.E. Rall, Nuclear hormone receptor CHR3 is a critical regulator of all four larval molts of the nematode *Caenorhabditis elegans*, Proc. Natl. Acad. Sci. USA 98 (2001) 7360–7365.
[11] J. Yochem, S. Tuck, I. Greenwald, M. Han, A gp330/megalin-related protein is required in the major epidermis of *Caenorhabditis elegans* for completion of molting, Development 126 (1999) 597–606.
[12] D.R. Brooks, P.J. Appleford, L. Murray, R.E. Isaac, An essential role in molting and morphogenesis of *Caenorhabditis elegans* for ACN-1, a novel member of the angiotensin-converting enzyme family that lacks a metallopeptidase active site, J. Biol. Chem. 278 (2003) 52340–52346.
[13] M.W. Davis, A.J. Birnie, A.C. Chan, A.P. Page, E.M. Jorgensen, A conserved metalloprotease mediates ecdysis in *Caenorhabditis elegans*, Development 131 (2004) 6001–6008.
[14] A.R. Frand, S. Russel, G. Ruvkun, Functional genomic analysis of *C. elegans* molting, PLoS Biol. 3 (2005) e312.
[15] E.A. Cox, J. Hardin, Sticky worms: adhesion complexes in *C. elegans*, J. Cell Sci. 117 (2004) 1885–1897.
[16] T.M. Rogalski, B.D. Williams, G.P. Mullen, D.G. Moerman, Products of the unc-52 gene in *Caenorhabditis elegans* are homologous to the core protein of the mammalian basement membrane heparan sulfate proteoglycan, Genes Dev. 7 (1993) 1471–1484.
[17] D.G. Moerman, B.D. Williams, Sarcomere assembly in *C. elegans* muscle, WormBook (2006) 1–16.
[18] R. Francis, R.H. Waterston, Muscle cell attachment in *Caenorhabditis elegans*, J. Cell Biol. 114 (1991) 465–479.
[19] M.C. Hresko, L.A. Schriefer, P. Shrimankar, R.H. Waterston, Myotactin, a novel hypodermal protein involved in muscle–cell adhesion in *Caenorhabditis elegans*, J. Cell Biol. 146 (1999) 659–672.
[20] J.M. Bosher, B.S. Hahn, R. Legouis, S. Sookhareea, R.M. Weimer, A. Gansmuller, A.D. Chisholm, A.M. Rose, J.L. Bessereau, M. Labouesse, The *Caenorhabditis elegans* vab-10 spectraplakin isoforms protect the epidermis against internal and external forces, J. Cell Biol. 161 (2003) 757–768.
[21] V. Hapiak, M.C. Hresko, L.A. Schriefer, K. Saiyasisongkhram, M. Bercher, J. Plenefisch, Mua-6, a gene required for tissue integrity in *Caenorhabditis elegans*, encodes a cytoplasmic intermediate filament, Dev. Biol. 263 (2003) 330–342.
[22] M. Bercher, J. Wahl, B.E. Vogel, C. Lu, E.M. Hedgecock, D.H. Hall, J.D. Plenefisch, Mua-3, a gene required for mechanical tissue integrity in *Caenorhabditis elegans*, encodes a novel transmembrane protein of epithelial attachment complexes, J. Cell Biol. 154 (2001) 415–426.
[23] L. Hong, T. Elbl, J. Ward, C. Franzini-Armstrong, K.K. Rybicka, B.K. Gatewood, D.L. Baillie, E.A. Bucher, MUP-4 is a novel transmembrane protein with functions in epithelial cell adhesion in *Caenorhabditis elegans*, J. Cell Biol. 154 (2001) 403–414.
[24] B.D. Williams, R.H. Waterston, Genes critical for muscle development and function in *Caenorhabditis elegans* identified through lethal mutations, J. Cell Biol. 124 (1994) 475–490.
[25] A.D. Chisholm, J. Hardin, Epidermal morphogenesis, WormBook (2005) 1–22.
[26] L. Broday, C.A. Hauser, I. Kolotuev, Z. Ronai, Muscle–epidermis interactions affect exoskeleton patterning in *Caenorhabditis elegans*, Dev. Dyn. 236 (2007) 3129–3136.
[27] S. Brenner, The genetics of *Caenorhabditis elegans*, Genetics 77 (1974) 71–94.
[28] J.D. Plenefisch, X. Zhu, E.M. Hedgecock, Fragile skeletal muscle attachments in dystrophic mutants of *Caenorhabditis elegans*: isolation and characterization of the mua genes, Development 127 (2000) 1197–1207.
[29] L. Broday, I. Kolotuev, C. Didier, A. Bhoumik, B. Podbilewicz, Z. Ronai, The LIM domain protein UNC-95 is required for the assembly of muscle attachment structures and is regulated by the RING finger protein RNF-5 in *C. elegans*, J. Cell Biol. 165 (2004) 857–867.
[30] C. Didier, L. Broday, A. Bhoumik, S. Israeli, S. Takahashi, K. Nakayama, S.M. Thomas, C.E. Turner, S. Henderson, H. Sabe, Z. Ronai, RNF5, a RING finger protein that regulates cell motility by targeting paxillin ubiquitination and altered localization, Mol. Cell. Biol. 23 (2003) 5331–5345.
[31] H. Iioka, S. Iemura, T. Natsume, N. Kinoshita, Wnt signalling regulates paxillin ubiquitination essential for mesodermal cell motility, Nat. Cell Biol. 9 (2007) 813–821.